

Gearless low-speed PMSM drive with estimator of perturbed rotor position angle

Streszczenie. W artykule przedstawiono system napędowy taśmociągu z wolnobieżnym silnikiem PMSM o mocy 250kW. Silnik został zoptymalizowany w kierunku osiągnięcia maksymalnej wartości momentu w obszarze przeciążenia. Zostało to osiągnięte między innymi poprzez wprowadzenie dodatkowych wypełnień z materiału ferromagnetycznego na obwodzie wirnika. Do wyznaczania położenia wirnika wykorzystano system estymacji bazujący na zakłóconym sygnale pomiarowym z enkodera absolutnego o komunikacji szeregowej SSI. Estymator położenia został zweryfikowany w układzie modelowym oraz rzeczywistym systemie napędowym. **System napędowy taśmociągu z wolnobieżnym silnikiem PMSM**

Abstract. The drive system of belt conveyor with low-speed PMSM motor rated at 250 kW is presented in the paper. The motor has been optimized so that it would attain maximum torque value in overload range. This has been achieved by introducing additional packing of ferromagnetic material along the rotor circumference. To determine rotor position, an estimation system basing on perturbed test signal from absolute encoder with SSI serial communication has been used. The position estimator has been verified in the model circuit and real drive system.

Słowa kluczowe: silniki PMSM, napęd wolnobieżny, sterowanie mikroprocesorowe

Keywords: PMSM, low-speed drive, microprocessor control

Introduction

In recent years permanent magnet motors are used more and more often in industrial applications. Even though these motors are more expensive, they are applied on account of such favourable features as higher efficiency, high overload capacity and possibility of obtaining significant torque at standstill [1,2].

In the range of medium- and high-power motors we encounter mostly permanent magnet synchronous motors (PMSM) characterized by sinusoidal emf. In order to control these motors properly, information on instantaneous rotor position relative to stator winding is required. This may be obtained by position measurement achieved with the help of encoder or by estimation of this position on the basis of other measured motor values [3].

The spectrum of PMSM applications is uncommonly extensive. These machines are used as generators in wind power plants [4] and hydropower plants, main and auxiliary drives in electric vehicles [5, 6, 7], locomotives, trams [8], ships [9]. The low-speed drives are among some very specific applications. In order to obtain relatively low mechanical speed, mechanical transmissions are usually used. The gear causes a decrease in the total efficiency of the drive, generates additional noise and may also constitute an extra source of failures [10]. It must be noted that induction cage motors with large numbers of pole pairs are characterized by low coefficient of power density (specific power). The existing gap is slowly bridged by permanent magnet synchronous motors [11]. Low-speed PMSMs are characterized by high number of pole pairs as well as feasible low rated frequency. Since they are supplied from frequency converters, this fact does not create any problem. We must emphasize another advantage exhibited by low-speed drives, i.e. decrease in the noise level; this is due to smaller number of rotating elements (gearless) as well as low speed of the drive.

The issues related to drive systems, including permanent motor drives, are widely represented in literature of the subject [12]. The control problems are addressed [3, 13] as well as performance characteristics such as motor efficiency [14]. For last several years, the subject of drive design utilizing low-speed motors is more and more extensively present in scientific publications [15]. The papers most often relate to a specific subject matter, such as typical uses of low-speed drives: motors built into wheels of electric vehicles [16, 17], lift drives [18] or pumps used in oil extraction [19]. The search for new optimum

designs encompasses also hybrid solutions, where motor and transmission functions are coupled in one electromagnetic entity [20].

The current article is focused on the belt conveyor drive, which uses a low-speed PMSM with reversed design instead of cage induction motor and transmission. Motor is rated at 250 kW, 1 kV and its rotor is integrated with drive drum of the conveyor. The potential application field is conveyor systems for bulk materials. This type of transport is common in heavy industry, mine industry and power engineering [21,22,23].

Low-speed PMSM

Nowadays the drive system of belt conveyors consists of motor, couplings/gear, mechanical transmission and drum. All elements except the drum are located apart from limiting outline of the conveyor. In order to reduce the space occupancy and to increase power efficiency, we have elaborated a new solution for the drive system, based upon low-speed PMSM, rated at 250 kW. This motor is built directly into the drive drum. The motor is fitted with external rotor, which constitutes an element of the drive drum casing. Due to this concept, it is possible to eliminate mechanical transmission from the drive system and any additional subassemblies are not mounted outside the conveyor itself [21]. This drive is presented in Fig.1a; a photo of the manufactured prototype of the motor built into the conveyor body is shown in Fig.1b.

The rated rotational speed of the motor is 45 rpm and this translates into linear speed of the belt equal to c. 3.2 m/s. The drive is supplied from frequency converter rated at 1000 V. The rated rotational torque of the motor is 53 kNm, and the maximum torque is 110 kNm. The power electronics supply makes it possible to control the rotational speed smoothly in the range of 0 to 55 rpm [22].

On account of reversed design of the motor (external rotor), it was necessary to work out the way of transmitting information on current rotational speed of the motor and rotor position relative to stator. A dedicated system of gears was designed, permitting the use of standard absolute encoder. The rotational speed is transmitted (with appropriate gear ratio) from the bearing plate to the encoder shaft; this is placed in easily accessible position inside the motor shaft. The motor is water-cooled. The main element of the system are channels placed beneath the stator laminations.

A most important feature of the belt conveyor drive is the maximum speed which may be attained by the motor. This is one of the key parameters influencing the suitability of the drive to the belt conveyor operation. For this reason, particular attention was paid to optimization of the electromagnetic circuit from the viewpoint of obtaining maximum torque. In standard electromagnetic circuits of machines with magnets placed upon the rotor core (surface-mounted permanent magnet - SPM), the space between neighbouring magnets is not filled up. However, by filling this space appropriately with ferromagnetic material it is possible to increase the value of torque for current values exceeding the rated value [22, 24]. Calculations were made using ANSYS Maxwell software, aimed at determination of optimum width of ferromagnetic pole piece between the magnets. The packing of the space (in percentage terms) between the magnets with ferromagnetic steel S355J2 was a parameter of the calculations. Analyzing the results, it may be noted that maximum electromagnetic torque is obtained for 60 to 75% filling of the space between the magnets with ferromagnetic material. The torque is higher by c. 12.3% in relation to the ferromagnetic-free design and by c. 2.5% in relation to spaces filled completely (100%) [22].

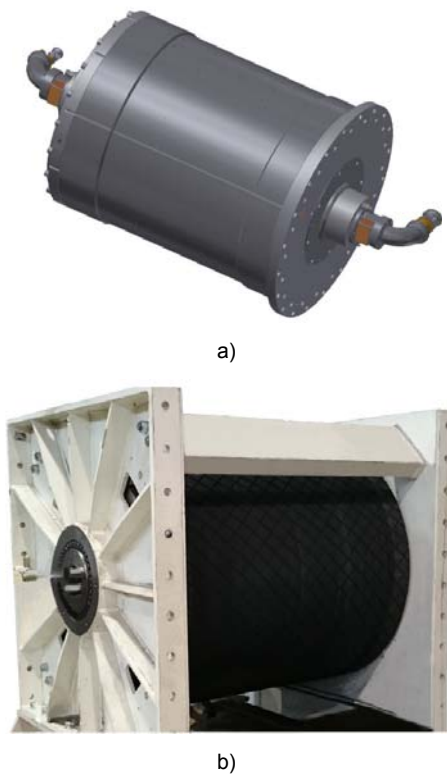


Fig. 1. PMSM rated at 250 kW and 45 rpm: a) rotor design b) photo of the motor

Figure 2 shows the dependency of the electromagnetic torque on current (current ranging from rated to near-maximum value) for 3 different variants of ferromagnetic filling: 0%, complete (100%) and optimum. It may be concluded from the results shown in Fig.2 that differences between obtained electromagnetic torque for the variant with the optimum filling of space between magnets and for other variants depend directly upon the current value (greater current-greater difference).

Power Electronics Converter

A system of converters was built to meet the project demands. They included frequency converter for PMSM

motor supply and frequency converter fitted with circuits for energy recuperation (energy was fed back to supply the cage induction machine loading the investigated drive). The tests could be run with dc circuits of both converters connected or with independent operation of the converters supplied from the network. All converters were designed for 1000 V network, their rated power was approximately equal to 250 kW and current overload was equal to double rated current. IGBT MBN800E33D transistors, manufactured by Hitachi, were used; their maximum blocking voltage is 3.3 kV and maximum current is 800 A. The serial water-cooling system is able to remove the heat losses effectively.

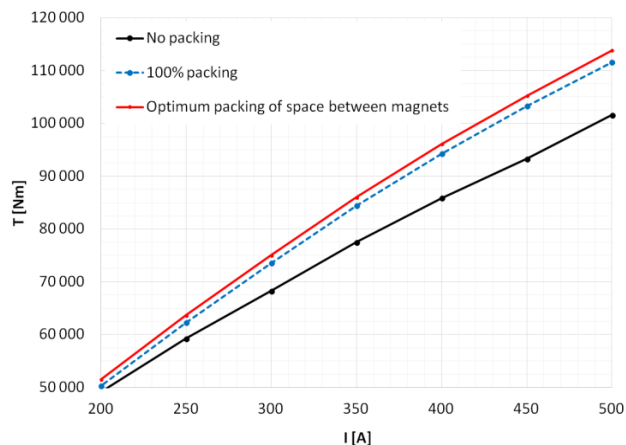


Fig.2. Electromagnetic torque vs. current for different variants of filling spaces between the permanent magnets

The control system of the converter for PMSM drive was based upon microcontroller TMS 320F28335. A significant advantage of this microcontroller is high data processing speed (150 MIPS) and enhanced control peripheral designed to meet the demands of power electronics converters. We may indicate here the ePWM blocks which can generate up to 12 signals controlling the transistors, enhanced eCAP and eQEP circuits dedicated to cooperation with incremental encoder, high-precision 16-channel 12-bit ADC and serial port peripherals. The control application was prepared in CCS integrated development environment and it contains all indispensable functional blocks for user interfaces, control algorithm, protection and diagnostics.

The control system of PMSM drive was based upon the well-known field-oriented method, where torque/current ratio is optimized. The block diagram of the control system is shown in Fig.3. The simulation characteristics of control angle vs. current were determined and written to non-volatile memory of the control system. The drive may operate with speed control or with set torque. The measurement processes, control procedures and SVM algorithm were synchronized with the switching frequency of inverter transistors, which was equal to 2.1 kHz. To generate control signals for inverter transistors three blocks of ePWM module were used; the leading block starts the operation cycle of A/D converter.

On account of essential reliability requirements of the drive and the need to obtain maximum torque from the very start, it has been assumed that the control system would use information on the rotor position. 13-bit absolute encoder manufactured by Kubler company was used; it is characterized by serial SSI communication protocol. In this way the number of connections between encoder and control system has been limited. This is important from the point of view of ensuring the intrinsic safety by galvanic isolation of signals.

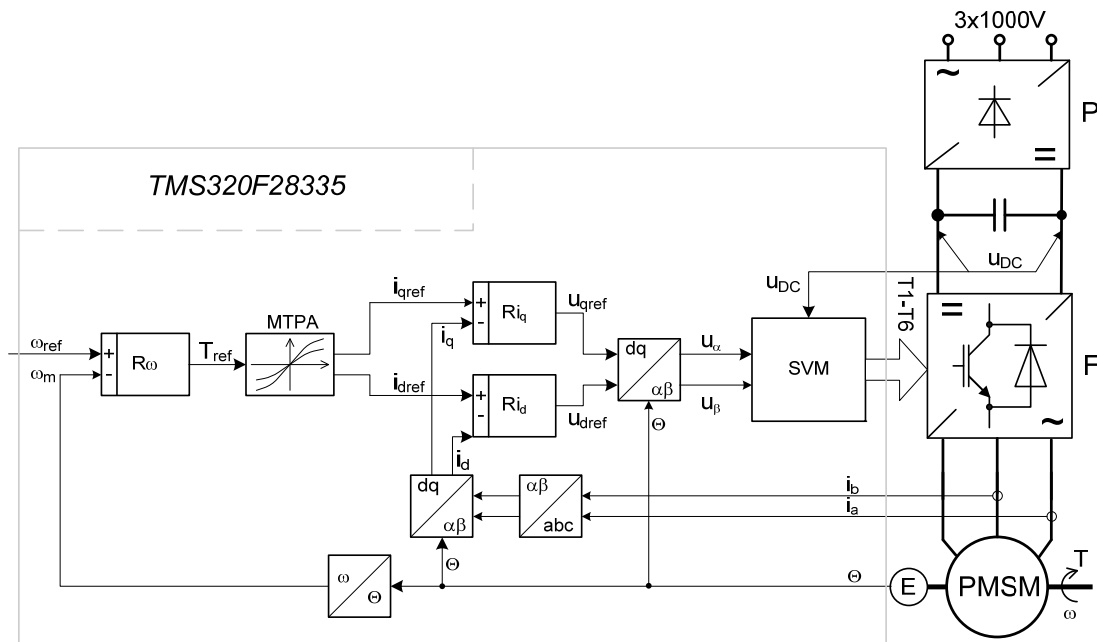


Fig. 3 Block diagram of low speed PMSM drive system control circuit

The connection of the reverse-design PMSM motor shaft required an appropriate gear, which permitted transmission of the rotor rotation to the encoder shaft. One turn of the rotor corresponded to number of turns of the encoder in accordance with the number of pole pairs, so that electrical angle of the motor matched the mechanical angle. The transmission of data using SSI protocol is unidirectional (from the encoder to the control system) and initiated by the microcontroller generating the clock signal $sclk$. The data sent $sdin$ is a 13-bit value of encoder position expressed in Gray code, it is not secured with any checksum. At least $15 \mu s$ must expire between end of transmission of one data block and beginning of transmission of another data block. The transmission circuit and supply circuit of the encoder are electrically separated. Transmission handling has been implemented using McBSP block of the microcontroller, in accordance with SSI protocol. This block makes it possible to emulate different modes of serial synchronous transmission. In this case the encoder position was read and then transmission took place, synchronous with the IGBT switching cycle. The subsequent communication cycles are shown in Fig.4. The information on the position gets to the McBSP buffer with a slight advance relative to beginning of interrupt service routine; the control system utilizes this information for carrying out transformation blocks. Due to this procedure, the delay between information on position and current readout and worked-out control has been minimized. Speed value was obtained in accordance with its definition. The cycle of speed measurement has been optimized in order to obtain appropriate dynamics and measurement precision.

The drive system was initially tested in laboratory. During tests a problem of incorrect encoder readings of the rotor position angle was encountered for motor speeds exceeding 30 rpm. The analysis showed that the erroneous readout occurred at the instant, when the encoder data block (to be precise: active slope of the first clock pulse) was correlated to IGBT switching.

During the switching cycle the data block position is constant, so the perturbation was observed only when motor speed was greater than given value, i.e. appropriate value of the 1st harmonic of the output voltage, when IGBT switching was synchronized with $sclk$ signal. This effect is

shown in Fig.5; the angle read from the encoder and transformed into analog value is also indicated. The motor rotated without load all the time, at speed equalling c. 40 rpm. It may be noted that erroneous readout of the angle caused incorrect calculation of values of current components i_q and i_d ; as a result, the output voltage of the inverter was also wrong. In this particular case the motor started to brake rapidly, which caused an increase in i_a current amplitude. This caused saturation of measurement current probe and increase in the converter's dc link circuit voltage, which in turn caused an increase in the u_{ab} voltage envelope.

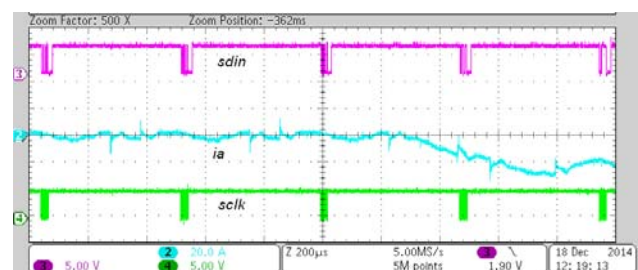


Fig. 4 Communication cycles between SSI encoder and inverter control circuit, $sclk$ - clock signal, $sdin$ - data, i_a - A phase current of the motor, $F_{switch} = 2,1 \text{ kHz}$

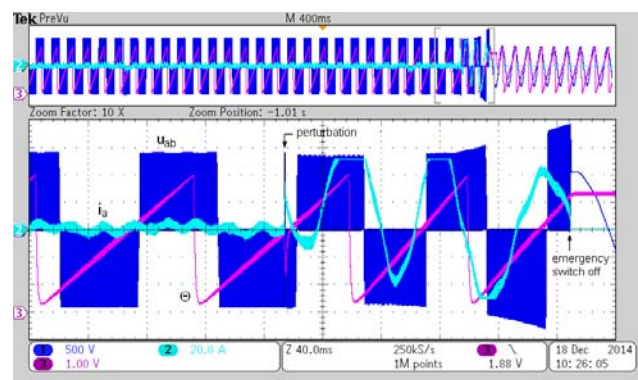


Fig. 5 Waveforms: voltage u_{ab} , PMSM current i_a and rotor position angle Θ with perturbed readout cycle

In the discussed case this perturbation led to emergency switch-off of the drive caused by uncontrolled electrical breaking and as a consequence exceedingly high value of U_{DC} voltage. A more thorough analysis of this particular erroneous readout showed that one of the clock pulses was omitted by the encoder and the read number was shifted by 1 bit. It cannot be ruled out that shifts by 2 or 3 bits could also be possible. Therefore analysis based exclusively on the principle of rejecting result divergent from the preceding one and correction of the readout data by 1 bit would not be effective. On account of synchronization of regulation (control) process and angle readout as well as analogous quantities (currents and voltages), a simple form of angle filtration is impossible, because this would require a multiple readout during one switching cycle and might not be effective after all.

Estimator of perturbed rotor position angle

In order to solve the problem presented above - incorrect readouts of the rotor position angle - the authors have proposed a new method, which makes it possible to estimate a correct value of the angle using the perturbed signal [24]. The block diagram of the circuit is shown in Fig.6. Two different modes of operation can be set by switching the contact S. When the perturbation source (frequency converter) does not operate, the readout of the position from encoder E is done in cycles and the value read is used directly. When the converter is on, the position angle is calculated in the estimation path by an adder: for each readout cycle the value from the preceding step is increased by the result generated by PI controller. The controller's task is to determine the value of angle increase between readout cycles. The controller's deviation is the difference between the readout angle θ and angle from the preceding step determined by the estimator $\theta_e(n-1)$. The deviation value (angle increase) is additionally limited in order to exclude values exceeding allowable limits (which are determined by maximum torque generated by the motor, its moment of inertia and cycle calculation time which is equal to the IGBT transistors' switching period). The increase of angle $\Delta\theta$ worked out by the estimator is a component of sum generating the estimated position $\theta_e(n)$ (together with the step value of preceding position). The value generated by the controller is limited by real values, the procedure is similar to the one mentioned earlier and adapted in case of deviation value. The preliminary values of the adder and part I of the controller are initially set during switching of contact S. This is done on the basis of earlier angle increments so that estimator operation should not undergo any undesirable perturbations.

The correctness of the estimator operation has been verified during tests of the model. The angle readouts from rotating encoder were subjected to the artificial perturbation generated by the control application. Two independent pseudorandom number generators were used; the first one generated bit value indicating whether the angle readout value were to be used or if it were to be overwritten with the value generated by the other pseudorandom generator. It has been assumed (on the basis of the practical experience of the drive) that number of perturbed readouts should not exceed 10%; in this way parameters of the first pseudorandom number generator have been determined. Generator #2 delivered angle values from the whole range of 13-bit number, the actual value was sampled in each computational step, regardless of further action adopted (i.e. whether this number was used or not). In order to eliminate the repeatability of the successive events during tests of the drive model, the initial value for the generator #1 was introduced as a time value from the

internal counter at the instant of drive start-up. On account of random performance of the operator switching the model on and off, the successive cycles of estimator operation were excited with different sequences of erroneous and correct angle readouts. During the tests the encoder rotated in the STOP mode of operation as well as during drive operating at different speeds and undergoing high dynamic changes set by model operator. These tests have let us determine the correct settings for estimator's PI controller and to verify the performance of the whole system.

In the second phase of the investigation the system has been tested in real drive with low-speed PMSM motor rated at 250 kW. The tests confirmed the encouraging properties of the estimator, which result in correct drive performance that is without perturbation which might lead to emergency switch-offs as well as possible deformations in current or reproduced rotor angle. Example of estimator operation is shown in Fig.7. Typical waveforms of rotor position angle are presented in the form of the analogue signal readout from the encoder, motor phase-to-phase voltages and encoder data obtained for rated speed of the motor. During 200 ms interval shown in the oscillogram (c. three periods of output voltage), three perturbed readout cycles may be observed; these have not caused any perturbances in motor supply voltage.

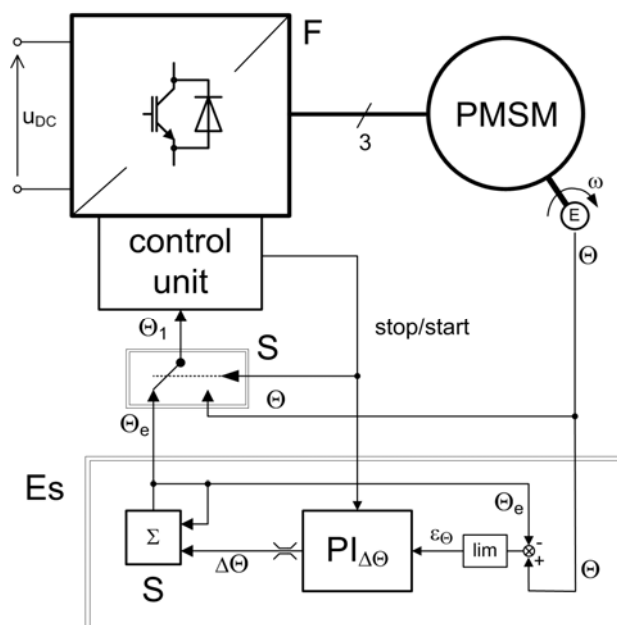


Fig. 6 Block diagram of angle estimation circuit

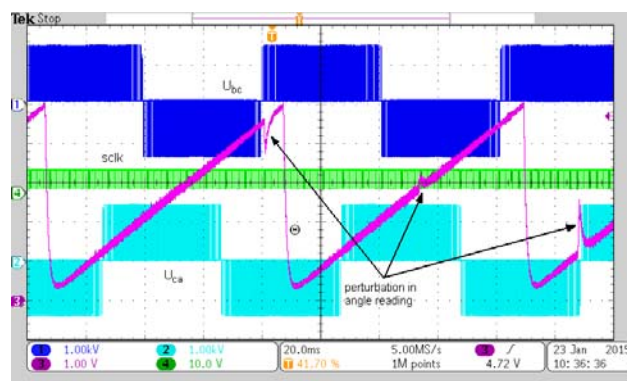
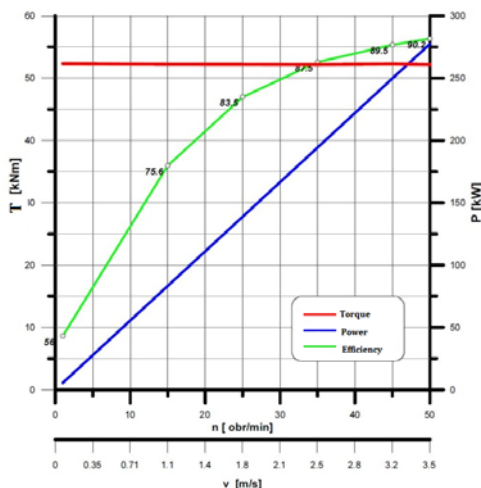


Fig. 7 Measured waveforms of voltages U_{bc} , U_{ca} , encoder signal $sclk$ and rotor position angle θ read directly from encoder, idle run, rotational speed equal to 45 rpm

a)



b)

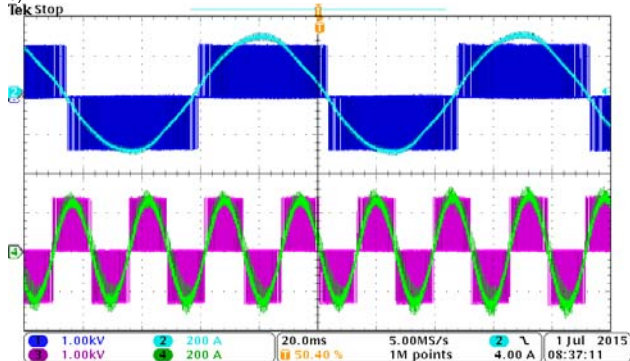


Fig. 8 Results of low-speed PMSM drive system tests: a) efficiency, torque and power curves, b) waveforms of phase-to-phase voltage and current of PMSM and induction load machine, rated operational conditions

Conclusion

The correctness of the PMSM drive performance has been verified by thermal tests. On account of high values of motor's thermal constants, these tests permitted proper verification of the adapted solution under real operating conditions. The motor worked continuously for more than 8 hours under rated conditions. Additionally it was also tested in the full range of operating speed and load torque. During successive tests we have not noted any perturbation in the motor operation, which might be caused by erroneous readout of the rotor position angle. Drive characteristics and total efficiency were determined during tests. Results are presented in Fig.8 as curves and current and voltage waveforms of PMSM motor and load machine.

Finally, the advantages of the designed drive must be emphasized, such as high efficiency, high starting torque and low noise level in particular. The low level of torque ripple at start-up or during dynamic states is also most important, especially in the belt conveyor drives operating under explosive conditions, since it increases the failure-free running time and in this way limits the expense of replacing high-quality conveyor belts.

Artykuł prezentuje wyniki związane ze zrealizowanym projektem współfinansowanym ze środków Europejskiego Funduszu Rozwoju Regionalnego w ramach Programu Operacyjnego Innowacyjna Gospodarka nr POIG.01.03.01-24-075/12, pt. „Bezprzekładniowy i wysokosprawny napęd elektryczny górniczego przenośnika taśmowego”



Authors:

dr inż. Tomasz Biskup
 E-mail: t.biskup@enel-pc.pl
 ENEL-PC sp. z o.o.
 ul. Graniczna 74B, 44-178 Przyszowice
 dr inż. Henryk Kołodziej
 E-mail: henryk.kolodziej@enel-pc.pl
 ENEL-PC sp. z o.o.
 ul. Graniczna 74B, 44-178 Przyszowice
 mgr inż. Tomasz Wolnik
 E-mail: t.wolnik@komel.katowice.pl
 Institute of Electrical Drives and Machines
 Al. Roździeńskiego 188, 40-203 Katowice
 mgr inż. Emil Król
 E-mail: e.krol@komel.katowice.pl
 Institute of Electrical Drives and Machines
 Al. Roździeńskiego 188, 40-203 Katowice

REFERENCES

- [1] Bose B. K.: Modern Power Electronics and AC Drives, Prentice Hall, 2002
- [2] Dukalski P., Rossa R., Dzikowski A.: Symulacje pracy napędu z silnikiem synchronicznym wzbudzanym magnesami trwałymi przeznaczonego do zastosowania w lokomotywie akumulatorowej typu Lea BM-12, *Maszyny Elektryczne. Zeszyty Problemowe*, 3/2016, pp. 7-12
- [3] Pacas M. : Sensorless Drives in Industry Application, *IEEE Ind. Electr. Magazine*, Jun. 2011
- [4] Zhang Z., Zhao Y., Qiao W., Qu L.: A Discrete-Time Direct Torque Control for Direct-Drive PMSG-Based Wind Energy Conversion Systems, *IEEE Tran. on Ind. Appl.*, Vol. 51, no. 4, Jul/Aug 2015
- [5] Ahmad M. Z., Sulaiman E., Haron Z. A., Kosaka T.: Preliminary Studies on a New Outer-Rotor Permanent Magnet Flux Switching Machine with Hybrid Excitation Flux for Direct Drive EV Applications, *International Conference on Power and Energy (PECon)*, 2-5 December 2012, Kota Kinabalu Sabah, Malaysia
- [6] Rossa R.: Zaawansowane rozwiązania techniczne w napędzie elektrycznym „E-KIT” dla miejskiego samochodu osobowego, *Maszyny Elektryczne. Zeszyty Problemowe*, 2/2014, pp. 145-149
- [7] Rossa R., Wolnik T.: Porównanie dwóch silników synchronicznych z magnesami trwałymi do pojazdu terenowego typu Quad z napędem elektrycznym, *Maszyny Elektryczne. Zeszyty Problemowe*, 100/2013, pp. 105-110
- [8] Peroutka Z., Zeman K., Krůs F., Kořta F.: New Generation of Trams with Gearless Wheel PMSM Drives: From Simple Diagnostics to Sensorless Control, *14th International Power Electronics and Motion Control Conference, EPE-PEMC 2010*, 6-8 September 2010, Ohrid, Republic of Macedonia
- [9] Chen H., Ait-Ahmed N., Zaïm E.H., Machmoum M.: Marine Tidal Current Systems: state of the art, *IEEE International Symposium on Industrial Electronics (ISIE)*, 28-31 May 2012 Hangzhou China
- [10] Meier F. : Permanent-Magnet Synchronous Machines with Non-Overlapping Concentrated Windings for Low-Speed Direct-Drive Applications, PhD thesis, Royal Institute of Technology, School of Electrical Engineering Electrical Machines and Power Electronics, Stockholm 2008.
- [11] Jahns T. M.: The Expanding Role of PM Machines in Direct-Drive Applications, *International Conference on Electrical Machines and Systems (ICEMS)*, 20 - 23 August 2011 Beijing, China
- [12] Finch J.W., Giaouris D.: Controlled AC Electrical Drives, *IEEE Tran. on Ind. Elect.*, Vol. 55, no. 2, Feb. 2008
- [13] Ming-Shi Huang, Chin-Hao Chen, Hsin-Hung Chou, Guen-Zheng Chen, Wen-Ko Tsai: An Accurate Torque Control of Permanent Magnet Brushless Motor using Low-resolution Hall-Effect Sensors for Light Electric Vehicle Applications, *IEEE Energy Conversion Congress and Exposition 15-19 Sep. 2013 15-19 Sep. 2013, Denver, USA*
- [14] de Almeida A.T., Ferreira F. J. T. E., Baoming G.: Beyond Induction Motors – Technology Trends to Move Up Efficiency, *IEEE Tran. on Ind. Appl.* Vol. 50, no 3, May/June. 2014

- [15] Yaojing F., Kai Y., Chenglin G.: Design and Optimization of External-Rotor Torque Motor, International Conference on Electrical Machines and Systems (ICEMS), 15-18 Nov. 2009 Tokyo Japan
- [16] Iyer K. L. V., Mukundan S., Dhulipati H., Mukherjee K., Minaker B., Kar N. C.: Design Considerations for Permanent Magnet Machine Drives for Direct-Drive Electric Vehicles, IEEE International Electric Machines & Drives Conference (IEMDC), 10-13 May 2015 Coeur d'Alene, ID, USA
- [17] Shi-Uk Chung, Seok-Hwan Moon, Dong-Jun Kim, Jong-Moo Kim: Development of a 20-Pole-24-Slot SPMSM With Consequent Pole Rotor for In-Wheel Direct Drive, IEEE Tran. on Ind. Electr., Vol. 63, no. 1, Jan. 2016
- [18] Cicalé S., Albin L., Parasiliti F., Villani M.: Design of a Permanent Magnet Synchronous Motor with Grain Oriented Electrical Steel for Direct-Drive Elevators, XXth International Conference on Electrical Machines (ICEM), 2-5 Sept. 2012 Marseille France
- [19] Bingyi Z., Sen W., Guihong F.: Design of High-power PMSM for Direct-drive Oil Drilling Mud Pump, International Conference on Electrical Machines and Systems (ICEMS), 20 - 23 August 2011 Beijing, China,
- [20] Tlali P. M., Gerber S., Wang R.-J.: Optimal Design of an Outer-Stator Magnetically Geared Permanent Magnet Machine, IEEE Tran. on Magn., Vol. 52, no. 2, Feb 2016
- [21] Wolnik T.: Bezprzekładniowy napęd elektryczny górniczego przenośnika taśmowego, Przegląd Górniczy, 7/2016, pp. 63-69
- [22] Wolnik T., Król E.: Optymalizacja obwodu elektromagnetycznego silnika do bezprzekładniowego napędu górniczego przenośnika taśmowego, Maszyny Elektryczne. Zeszyty Problemowe, 2/2016 (110), pp. 123-128
- [23] Gawron S.: Wybrane innowacyjne projekty maszyn elektrycznych z magnesami trwałymi i ich praktyczne zastosowania, Maszyny Elektryczne. Zeszyty Problemowe, 1/2016 (109), pp. 1-10
- [24] Wolnik T., Król E., Glinka T., Białas A.: Silnik z magnesami trwałymi o zwiększonym momencie elektromagnetycznym, Patent RP nr PL226450 z dnia 31.07.2017
- [25] Biskup T., Kołodziej H., Glinka T., Wolnik T. : Sposób odtwarzania kąta położenia wirnika na podstawie informacji z enkodera absolutnego, Patent RP nr PL225493 z dnia 28.04.2017.